



HAL
open science

Contribution of the MP2RAGE 7T Sequence in MS Lesions of the Cervical Spinal Cord

B. Testud, N. Fabiani, S. Demortière, S. Mchinda, N.L. Medina, J. Pelletier,
M. Guye, B. Audoin, J.P. Stellmann, Virginie Callot

► **To cite this version:**

B. Testud, N. Fabiani, S. Demortière, S. Mchinda, N.L. Medina, et al.. Contribution of the MP2RAGE 7T Sequence in MS Lesions of the Cervical Spinal Cord. American Journal of Neuroradiology, 2023, 10.3174/ajnr.A7964 . hal-04193013

HAL Id: hal-04193013

<https://amu.hal.science/hal-04193013>

Submitted on 31 Aug 2023

HAL is a multi-disciplinary open access archive for the deposit and dissemination of scientific research documents, whether they are published or not. The documents may come from teaching and research institutions in France or abroad, or from public or private research centers.

L'archive ouverte pluridisciplinaire **HAL**, est destinée au dépôt et à la diffusion de documents scientifiques de niveau recherche, publiés ou non, émanant des établissements d'enseignement et de recherche français ou étrangers, des laboratoires publics ou privés.



Distributed under a Creative Commons Attribution 4.0 International License

Contribution of the MP2RAGE 7T sequence in multiple sclerosis lesions of the cervical spinal cord

Authors:

Benoit Testud, MD^{1,2*}; Noeline Fabiani^{1,2}, MD; Sarah Demortière, MD^{1,2,3}; Samira Mchinda^{1,2}, PhD^{1,2}; Nilser Laines Medina, PhD^{1,2}; Jean Pelletier, MD-PhD^{1,2,3}; Maxime Guye, MD-PhD^{1,2}; Bertrand Audoin, MD-PhD^{1,2,3}; JP Stellmann, MD^{1,2}; Virginie Callot, PhD^{1,2}

Affiliations :

¹Aix-Marseille Univ, CNRS, CRMBM, Marseille, France

²APHM, Hôpital Universitaire Timone, CEMEREM, Marseille, France

³APHM, Hôpital Universitaire Timone, Department of Neurology, Marseille, France

* Corresponding author:

Benoit Testud

Benoit.testud@ap-hm.fr

ORCID: 0000-0003-1444-3702

Fundings:

This work was supported by the ARSEP Foundation (Fondation pour l'Aide à la recherche sur la Sclérose en Plaques) and CNRS (Centre National de la Recherche Scientifique). It was performed within a laboratory member of France Life Imaging network (grant ANR-11-INBS-0006), on the platform 7T-AMI, a French "Investissements d'Avenir" programme (grant ANR-11-EQPX-0001).

Key words:

Ultra-high field imaging; Multiple sclerosis; spinal cord; MP2RAGE

Acknowledgments

The authors would like to thank Veronique Gimenez, Lauriane Pini, Claire Costes, Pierre Durozard, Audrey Rico, Adil Maarouf and Marie-Pierre Ranjeva for study logistics; as well as Tobias Kober from Siemens Healthcare for MR sequence support.

Abstract

Background and purpose

The detection of spinal cord lesions in multiple sclerosis patients is challenging. Recently, the 3D-MP2RAGE sequence demonstrated its usefulness at 3T. Benefiting from the high spatial resolution provided by ultra-high field MR systems, the objective of this work was to evaluate the contribution of the 3D-MP2RAGE sequence acquired at 7T for the detection of multiple sclerosis lesions in the cervical spine.

Materials and methods

Seventeen MS patients participated in this study. They were examined at both 3T and 7T. MR imaging examination included a MAGNIMS protocol with an axial T2*GRE-WI sequence (named “optimized MAGNIMS protocol”) and a 0.9-mm isotropic 3D-MP2RAGE sequence at 3T, as well as a 0.7-mm isotropic and 0.3-mm in-plane resolution anisotropic 3D-MP2RAGE sequences at 7T. Each dataset was read by a consensus of radiologists, neurologist, and neuroscientists. The number of lesions and their topography, as well as the visibility of the lesions from one set to another, were carefully analyzed.

Results

A total of 55 lesions were detected. The absolute number of visible lesions differed between the 4 sequences (LME anova $p=0.020$). Highest detection was observed for the two 7T sequences, with 51 lesions each (92.7% of the total). Optimized 3T MAGNIMS protocol and 3T MP2RAGE isotropic sequence detected 41 (74.5%) and 35 lesions (63.6%), respectively.

Conclusion

7T MP2RAGE sequences detected more lesions than 3T sets. Isotropic and anisotropic acquisitions performed comparably. Ultra-high resolution obtained at 7T improves the identification and delineation of lesions of the cervical spinal cord in multiple sclerosis.

Key words: Ultra-high field imaging; Multiple sclerosis; spinal cord; MP2RAGE

Introduction

Multiple sclerosis is an immune-mediated disease that is responsible for the formation of demyelinating lesions of the central nervous system, in which spinal cord involvement is very common (80% to 90%¹ of diagnosed patients) and responsible for a large portion of the disability^{2,3}. Lesion assessment within the spinal cord, which is one of the four locations to confirm temporal and spatial dissemination⁴, is thus crucial for the diagnosis of MS and for eliminating various differential diagnoses. The Magnetic Resonance Imaging in Multiple Sclerosis (MAGNIMS) guidelines⁵ recommend the study of the entire spinal cord using at least two MR sequences (e.g. sagittal T2-WI, proton density-weighted or STIR sequences, and/or T1-WI post-gadolinium) to increase the confidence in lesion detection. Axial T2-WI or T2*-WI sequences are also proposed to corroborate, characterize, or confirm the presence of visible lesions. Indeed, previous studies demonstrated their significant value for both improved lesion detection and confidence in the interpretation⁶⁻⁸.

In practice, lesion detection in the spinal cord of patients with MS is difficult and challenging even using 3T MRI scans. These difficulties are related to physiological noise such as breathing or cerebro-spinal fluid flow⁹ and to the relatively low spatial resolution of sequences acquired at lower field strengths such as 1.5 and 3T resulting in partial volume effects. Thanks to the increase in both signal-to-noise ratio (SNR) and contrast-to-noise ratio (CNR), ultra-high field magnetic resonance imaging at 7T of the cervical spinal cord now allows for a higher spatial resolution and more defined anatomical details^{10,11}, which can help detect and delineate cervical spinal MS lesions as compared to 3T evaluation^{11,12}. 7T reveals also information about lesion distribution in the spinal cord¹³. In the meantime, Demortière et al¹⁴ illustrated the value of the 3D-Magnetization Prepared 2 Rapid Acquisition Gradient Echo

(MP2RAGE)¹⁵ sequence at 3T, which allowed the detection of a greater number of MS lesions than sequences recommended by the MAGNIMS consensus. The MP2RAGE sequence has been used broadly on the brain^{16,17} and was more recently optimized for the cervical spinal cord at both 3T and 7T^{18,19}.

In line with these results, our goal was to determine the potential added value of the 7T 3D-MP2RAGE sequence over 3T MR evaluation for detecting cervical spinal cord lesions in patients with MS.

Materials and methods

Population

We analysed data collected from a prospective study focusing on the 3 and 7 Tesla multimodal assessment of spinal cord in MS that took place from December 2017 to September 2019. The study was approved by the local ethics committee and written informed consent was collected from each participant prior to the MR examinations. Inclusion criteria were a diagnosis of MS according to the revised McDonald 2017 criteria⁴, patients older than 18 years, clinical symptoms suggesting spinal cord involvement, and MR imaging examination performed at least 3 months after steroid infusion. Patients with uncertain diagnosis, in relapse, or with a standard contraindication to an MR examination such as incompatible implanted equipment, claustrophobia, agitation, intrabody metal fragments, were excluded.

Image acquisition

All MR examinations were performed on the same day using a 3T (Verio, Siemens Healthineers, Erlangen, Germany) and 7T (Magnetom, Siemens Healthineers, Erlangen, Germany) MR systems. MR imaging at 3T was performed using the body

coil for transmission and standard 12- channel head, 4-channel neck, and 24-channel spine matrix array coils for reception. MR imaging at 7T was performed using a customized 8Tx/8Rx transceiver coil array (Rapid Biomedical), used in CP mode. The 7T examination was performed in the morning and the 3T examination in the afternoon. The 3T MR protocol included the sequences recommended by the MAGNIMS consensus²⁰, i.e. sagittal 2D-T2-TSE-WI and STIR-WI, as well as an axial 2D-T2*-multiecho-GRE-WI sequence, hence forming an “optimized MAGNIMS” set. The 3T protocol also included one sagittal 3D-MP2RAGE sequence with isotropic resolution $(0.9 \text{ mm})^3$, which covered both brain and cervical spinal cord¹⁸, and provided two contrasted images (T11, T12), from which a uniform (UNI) image and a T1 map were derived.

At 7T, the MR protocol included an axial 3D-MP2RAGE sequence with a spatial resolution of $0.3 \times 0.3 \times 4 \text{ mm}^3$, and a coronal 3D-MP2RAGE sequence with an isotropic spatial resolution of $(0.7 \text{ mm})^3$. To locate the vertebral level on the 3D-MP2RAGE anisotropic sequence, a fast T2-TSE sequence was also performed. The main sequence parameters are summarized in the Table 1.

Magnetic Field	3T				7T	
Sequence	T2*-WI	T2-WI	STIR-WI	MP2RAGE	MP2RAGE ISOTROPIC	MP2RAGE ANISOTROPIC
Dimension / Orientation	2D Axial	2D Sagittal	2D Sagittal	3D Sagittal	3D Coronal	3D Axial
TR (s)	0.5	4	3.2	4	5	5
TE (ms)	27	113	53	2.48	2.15	3.05
FOV (mm)	180	280	320	300	260	256
Resolution (mm ³)	0.5 x 0.5 x 5	1.1 x 0.9 x 2	0.9 x 0.7 x 3	0.9 x 0.9 x 0.9	0.7 x 0.7 x 0.7	0.3 x 0.3 x 4
Slices	9 per slab, 2 slabs *			176	192	64 slices per slab, 1 or 2 slabs *, **
Acq. time (min)	5.26	1.54	2.18	7.18	8.47	6.02/slab

Table 1 - Main sequence parameters. * placed perpendicular to the cord, ** depending on cord curvature

Lesion Detection and Scoring

Lesion detection was performed by a consensus composed of a senior neuroradiologist (**), a senior neurologist (**), a neuroradiologist resident (**), and 3 neuroscientists specialized in spinal cord MRI and multiple sclerosis (**; **; **), all blinded to clinical data, using the HOROS Viewer (<https://horosproject.org>).

Each set (Optimized MAGNIMS, 3T MP2RAGE, 7T MP2RAGE with isotropic resolution and 7T MP2RAGE with anisotropic resolution) was viewed successively and individually by the reading group with a three-week delay between each session and the viewing order of the subjects was randomly generated for each set to avoid memory bias. 3T sequences were observed before 7T sequences to avoid potential learning biases on 3T images due to more informative 7T images. Finally, once all imaging sets had been observed, the 4 imaging sets were displayed simultaneously to obtain a lesion concordance between imaging sets. The UNI image and/or the T1

map of the 3D-MP2RAGE sequences were used for interpretation. Lesions visible on at least two consecutive slices, and whose radiological characteristics were in favor of MS lesions, were retained for the lesion count. For each lesion, the vertebral level (from C1 to C7), the location in the transverse section plane (anterior, lateral, posterior), and the involvement of the white and/or gray matter, were recorded. Lesions in front of the intervertebral disc were considered to belong to the overlying level.

Statistics

We performed descriptive statistics on the cohort and compared the total number of lesions visualized per sequence. We compared the absolute number of visible lesions over all sequences by computing the anova of a linear mixed effect (LME) model accounting for recurrent measurements in patients. We also computed the dice score for pairwise comparisons as an indicator of the similarity. The LME approach was also applied to explore differences between spinal cord levels. P-values below 0.05 were considered significant. All statistical analyses were performed using R (<http://www.r-project.org>).

Results

Population

Of the 19 patients, 2 were excluded because the spinal cord presented with inseparable lesions (diffuse aspect). Consequently, 17 patients participated in the study (12 women / 5 men; (mean age; range) 30.2 ± 9.9 years [20 – 41]), all had a relapsing-remitting form of the disease. The study population presented with a mild disability, with a median EDSS score was 1.5 (mean of 0.9 ± 1 [0 – 3]) and a short

disease duration with a median of 17 months (mean 40.8 ± 47.3 ; [6 – 189]). Six patients in the study had no therapy. Detailed demographic data, clinical characteristics and lesion counts, reported as the maximum number of lesions visualized in each patient, are summarized in Table 2. The 7T isotropic resolution 3D-MP2RAGE sequence was missing for 3/17 patients.

Patients	Age (years)	Sex	Disease course	Disease duration (months)	EDSS	Lesion count
P1	40	M	RR	95	2	7
P2*	20	F	RR	58	2,5	3
P3	30	F	RR	87	1,5	6
P4	27	F	RR	17	3	6
P5	23	F	RR	47	0	5
P6	31	F	RR	6	0	0
P7	35	F	RR	33	1	3
P8	28	F	RR	6	0	3
P9	38	F	RR	7	1	0
P10	33	M	RR	17	0	3
P11	31	F	RR	189	0	12
P12	41	F	RR	45	1	7
P13	26	M	RR	12	0	3
P14	20	M	RR	44	0	0
P15	30	F	RR	10	1	0
P16*	35	M	RR	11	2	12
P17*	26	F	RR	10	1	8

Table 2: Demographic and clinical characteristics. M: Male, F: Female, RR: relapsing-remitting, EDSS: Expanded Disability Status Scale, * indicates the patients who could not have the examination with the 7T isotropic MP2RAGE sequence.

Lesion characteristics

Four patients presented with no lesions. Among the 14 patients who had a complete four sets of images, 55 lesions were identified in total, 31 located in the posterior part of the spinal cord (56.4%), 17 lateral (30.9%), 6 anterior (10.9%) and one central.

Twenty-eight lesions (50.9%) affected the white matter only, the remaining affected both white and gray matter. Figure 1 shows the proportion of lesions detected by each sequence on the spinal cord globally, and for each level, considering only the patients who had all 4 imaging sets. The absolute number of visible lesions differed between the 4 sequences (LME anova $p = 0.020$). Highest detection was observed for the two 7T sequences with 51 lesions each (LME anova $p = 1$, dice = 0.92).

Detection at 7T was higher on average (whole cervical cord considered) than at 3T (LME anova 3T vs 7T $p = 0.003$, dice = 0.59). Figures 2 to 5 show examples of lesions that were only visible at 7T. For the 3T MP2RAGE isotropic sequence, 35 lesions were detected (dice = 0.57), which was not significantly less than the optimized MAGNIMS protocol with 41 lesions (dice = 0.61, LME anova $p = 0.239$). The spatial distribution of lesions showed the highest absolute numbers at C2, C3 and C5 levels.

Concerning patients who could not have the examination with the 7T isotropic MP2RAGE sequence, the highest lesion detection was with the 7T anisotropic sequence with 23 lesions. 3T MP2RAGE and optimized MAGNIMS performed similarly with 15 lesions detected each.

Among all patients in the cohort, 8/78 lesions (10%) were not detected at 7T, 4 with the 7T MP2RAGE anisotropic and 4 with the 7T MP2RAGE isotropic sequences. For 3 lesions, this was related to artifacts that interfered with the lesion detection. For the 5 remaining lesions, this was related to having too low spatial resolution: 3 lesions were not detected on the 7T MP2RAGE isotropic sequence but were visible on the 7T MP2RAGE anisotropic sequence, and 2 lesions that had a very small diameter in the sagittal and coronal plane were not seen on the 7T MP2RAGE anisotropic sequence due to slice thickness partial volume effects, but were visible on the 7T MP2RAGE isotropic sequence.

Discussion

This study showed promising results on the contribution of ultra-high field (7T) 3D-MP2RAGE sequences to cervical spinal cord involvement in MS. In addition, it provides several useful comments for clinical research practice.

In line with the literature¹¹, the expected increase in CNR and SNR at ultra-high field¹⁰ and the high resolution allowed detection of a greater number of lesions than at 3T. The study additionally provides an objective 3-7T comparison using the MP2RAGE sequence, compared to Dula et al¹¹ which compared slightly different contrasts (7T T2*-WI FFE versus 3T T2-WI FSE axial sequences). The readers experienced an improved viewing even in the case of numerous and coalescing lesions at 7T compared to 3T. 7T 3D-MP2RAGE allows better lesion delineation leading to a more accurate and reliable counting compared to 3T imaging sets. The readers were able on several occasions to easily confirm the presence of hardly visible lesions or lesions referred to as nonspecific signal anomalies on 3T images, even for an inexperienced reader. Among the patients who had the two 7T

MP2RAGE sequences, we did not observe any difference in terms of detection. All visible lesion at 3T were identified on one of the two 7T sets and only 8 lesions visible at 3T were not seen on one of the two 7T sets in the entire cohort. Not detecting lesions at 7T was due to artefacts or very small lesions in the z-axis (resp. transverse) plane, which penalized the 7T MP2RAGE anisotropic (resp. 7T MP2RAGE isotropic) sequence. It should be noted that the 7T 3D-MP2RAGE sequence with isotropic resolution, which had a long acquisition time, was acquired last in our protocol, which potentially made it more vulnerable to motion artefacts. Considering the 3T datasets, Demortiere et al¹⁴ previously reported an improved lesion detection using the 3T MP2RAGE sequence as compared to the conventional MAGNIMS set. In our protocol, an “optimized” MAGNIMS set including an axial 2D T2*GRE-WI sequence, providing high in-plane axial resolution (0.5 mm) with high white matter / gray matter / lesion contrast, was used instead. Despite being considered as optional according to the latest guidelines⁵, the T2*GRE-WI sequence nonetheless allowed the detection of many lesions not visible otherwise, thus explaining the relative success of our optimized MAGNIMS as compared to the 3T MP2RAGE. The relatively poor performance of 3T sequences at C4 level may be attributed to the acquisition of the T2*-WI sequence in two slabs, where C4 constitutes the interface between the slabs. This may have interfered with the viewing. No specific reason was identified for the 3T MP2RAGE sequence and this should be further investigated in larger cohort. An objective comparison between 2D T2*GRE-WI, MP2RAGE and the conventional MAGNIMS set at 3T was beyond the scope of the present study. However, such comparison may be of interest in the future as the 3D-MP2RAGE sequence offers a shorter acquisition time than the optimized MAGNIMS, as well as a simultaneous coverage of both brain and cervical

cord¹⁸ with an isotropic resolution. It would thus be particularly relevant for MS and may be a good alternative to the MAGNIMS set in clinical practice.

Regarding the lesion location, lesions were more frequent in upper cervical cord (C2-C3), and lesions in the posterior and lateral cords were the most numerous, which is in agreement with the literature^{21,22}.

No specific radiological pattern was better detected at 7T than at 3T. However, the gain in contrast and resolution allowed the detection of small lesions, in locations that were not easily accessible at 3T, such as the anterior cord or on the outer edge of the cord in contact with the cerebrospinal fluid. In addition, readers experienced a learning effect of imaging at 7T, i.e., some lesions not reported at 3T could subsequently be retained after the 7T reading. Lefeuvre et al²³ were able to establish the existence of sub-pial white matter lesions using an animal experimental autoimmune encephalomyelitis model of the spinal cord, which has not been reported so far in the human spinal cord. These lesions were revealed by ex vivo ultra-high resolution 7T MRI (3D T2*-WI with an in-plane resolution of 70 μm and a slice thickness of 200 μm), and thus unrevealable by our study.

Within this study, we chose to focus on the MP2RAGE sequence, which was shown to be more robust. While the T2*-WI of the spinal cord at 7T is a high reward sequence with a high resolution and a high contrast for lesion detection^{11,13,23}, it is also a high risk sequence, which is sensitive to inhomogeneities of the magnetic field and to motion artefacts²⁴.

Our study has several limitations. It is a retrospective study with a small sample size. Although our lesion features are comparable to those in the literature and provide a

representative sample of spinal cord injury in multiple sclerosis, a further study with a larger sample size is needed to confirm our results.

The learning effect on readers may also be a potential bias in this work, which may have led to an improvement in the performance of the readers. Nonetheless, we assume this was minimized by interpreting the images in different sessions with a minimum interval of three weeks and presenting the patients in a random order.

For each patient the 7T MR exam was performed first and this may have benefited the 7T evaluation by having less risk of motion artifacts than the 3T evaluation performed later. However, patients had a long break between the two exams, which limited this bias. Lastly, our reading process didn't allow for reporting of individual confidence, nor did we perform a concordance between readers, which may limit the relevance of our results. Nevertheless, it allowed to establish a level-by-level lesion concordance between imaging sets.

From a practical point of view, 7T sequences detected more lesions than 3T sequences. However, this added value in lesion detection must be balanced with a potentially longer acquisition time. While the 3T MP2RAGE sequence seems to be an interesting alternative to the MAGNIMS set with a T2* axial sequence, given the equivalent acquisition time, similar lesion detection and the possibility of covering the brain (included in the FOV), the 7T sequences are more oriented towards more precise indications. For example, the use of the 7T MP2RAGE sequence with ultra-high resolution in axial plane could find its place beyond multiple sclerosis in the fine characterization of cervical myelitis or to better appreciate possible doubtful lesions.

In conclusion, thanks to increased spatial resolution, 7T 3D-MP2RAGE sequences allowed for improved identification and delineation of lesions as compared to 3T.

It would be interesting to study longitudinally the potential impact of the 7T MP2RAGE sequences on the management of multiple sclerosis patients.

The clinical research perspectives of 7T MRI now require technical advances, to image the thoracic and lumbar spinal cord, and to reduce the acquisition time in implementing a "compressed-sensing" version of the method²⁵ for the cord.

Whilst waiting for the full development and greater availability of 7T systems, it could also be interesting to investigate further the potential of the 3T 3D-MP2RAGE protocol dedicated to both brain and cervical spinal cord as an alternative to the conventional MAGNIMS protocol.

Acknowledgments

The authors thank V.Gimenez, L.Pini, C.Costes, P. Durozard, A. Rico, A. Maarouf and M.P. Ranjeva for study logistics, as well as Tobias Kober from Siemens Healthcare for MR sequence support.

Fundings

This work was supported by the ARSEP Foundation (Fondation pour l'Aide à la recherche sur la Sclérose en Plaques) and CNRS (Centre National de la Recherche Scientifique). It was performed within a laboratory member of France Life Imaging network (grant ANR-11-INBS-0006), on the platform 7T-AMI, a French "Investissements d'Avenir" programme (grant ANR-11-EQPX-0001).

References

1. Bot JCJ, Blezer ELA, Kamphorst W, et al. The Spinal Cord in Multiple Sclerosis: Relationship of High-Spatial-Resolution Quantitative MR Imaging Findings to Histopathologic Results. *Radiology* 2004;233:531–40.
2. Gass A, Rocca MA, Agosta F, et al. MRI monitoring of pathological changes in the spinal cord in patients with multiple sclerosis. *The Lancet Neurology* 2015;14:443–54.
3. Brownlee WJ, Altmann DR, Prados F, et al. Early imaging predictors of long-term outcomes in relapse-onset multiple sclerosis. *Brain* 2019;142:2276–87.
4. Thompson AJ, Banwell BL, Barkhof F, et al. Diagnosis of multiple sclerosis: 2017 revisions of the McDonald criteria. *The Lancet Neurology* 2018;17:162–73.
5. Wattjes MP, Ciccarelli O, Reich DS, et al. 2021 MAGNIMS–CMSC–NAIMS consensus recommendations on the use of MRI in patients with multiple sclerosis. *The Lancet Neurology* 2021;20:653–70.
6. Weier K, Mazraeh J, Naegelin Y, et al. Biplanar MRI for the assessment of the spinal cord in multiple sclerosis. *Mult Scler* 2012;18:1560–9.
7. Galler S, Stellmann J-P, Young KL, et al. Improved Lesion Detection by Using Axial T2-Weighted MRI with Full Spinal Cord Coverage in Multiple Sclerosis. *American Journal of Neuroradiology* 2016;37:963–9.
8. Bergers E, Bot JCJ, De Groot CJA, et al. Axonal damage in the spinal cord of MS patients occurs largely independent of T2 MRI lesions. *Neurology* 2002;59:1766–71.
9. Stroman PW, Wheeler-Kingshott C, Bacon M, et al. The current state-of-the-art of spinal cord imaging: Methods. *NeuroImage* 2014;84:1070–81.
10. Barry RL, Vannesjo SJ, By S, et al. Spinal cord MRI at 7T. *NeuroImage* 2018;168:437–51.
11. Dula AN, Pawate S, Dortch RD, et al. Magnetic resonance imaging of the cervical spinal cord in multiple sclerosis at 7T. *Mult Scler* 2016;22:320–8.
12. Kreiter DJ, van den Hurk J, Wiggins CJ, et al. Ultra-high field spinal cord MRI in multiple sclerosis: Where are we standing? A literature review. *Multiple Sclerosis and Related Disorders* 2022;57:103436.
13. Ouellette R, Treaba CA, Granberg T, et al. 7 T imaging reveals a gradient in spinal cord lesion distribution in multiple sclerosis. *Brain* 2020;143:2973–87.
14. Demortière S, Lehmann P, Pelletier J, et al. Improved Cervical Cord Lesion Detection with 3D-MP2RAGE Sequence in Patients with Multiple Sclerosis. *AJNR Am J Neuroradiol* 2020;41:1131–4.
15. Marques JP, Kober T, Krueger G, et al. MP2RAGE, a self bias-field corrected sequence for improved segmentation and. *Neuroimage* 2010;49:1271–81.
16. Okubo G, Okada T, Yamamoto A, et al. MP2RAGE for deep gray matter measurement of the brain: A comparative study with MPRAGE: MP2RAGE for Deep Gray Matter Measurement. *J Magn Reson Imaging* 2016;43:55–62.
17. Marques JP, Gruetter R. New Developments and Applications of the MP2RAGE Sequence - Focusing the Contrast and High Spatial Resolution R1 Mapping. Yacoub E, ed. *PLoS ONE* 2013;8:e69294.
18. Forodighasemabadi A, Rasoanandrianina H, El Mendili MM, et al. An optimized MP2RAGE sequence for studying both brain and cervical spinal cord in a single acquisition at 3T. *Magnetic Resonance Imaging* 2021;84:18–26.
19. Massire A, Taso M, Besson P, et al. High-resolution multi-parametric quantitative magnetic resonance imaging of the human cervical spinal cord at 7T.

NeuroImage 2016;143:58–69.

20. Filippi M, Rocca MA, Ciccarelli O, et al. MRI criteria for the diagnosis of multiple sclerosis: MAGNIMS consensus guidelines. *The Lancet Neurology* 2016;15:292–303.

21. Eden D, Gros C, Badji A, et al. Spatial distribution of multiple sclerosis lesions in the cervical spinal cord. *Brain* 2019;142:633–46.

22. Kearney H, Miller DH, Ciccarelli O. Spinal cord MRI in multiple sclerosis—diagnostic, prognostic and clinical value. *Nat Rev Neurol* 2015;11:327–38.

23. Lefeuvre JA, Guy JR, Luciano NJ, et al. The spectrum of spinal cord lesions in a primate model of multiple sclerosis. *Mult Scler* 2020;26:284–93.

24. Frebourg G, Massire A, Pini L, et al. The good, the bad and the ugly : a retrospective study of human cervical spinal cord image quality at 7T. *ISMRM meeting 2021*.

25. Mussard E, Hilbert T, Forman C, et al. Accelerated MP2RAGE imaging using Cartesian phyllotaxis readout and compressed sensing reconstruction. *Magn Reson Med* 2020;84:1881–94.

FIGURES AND TABLES

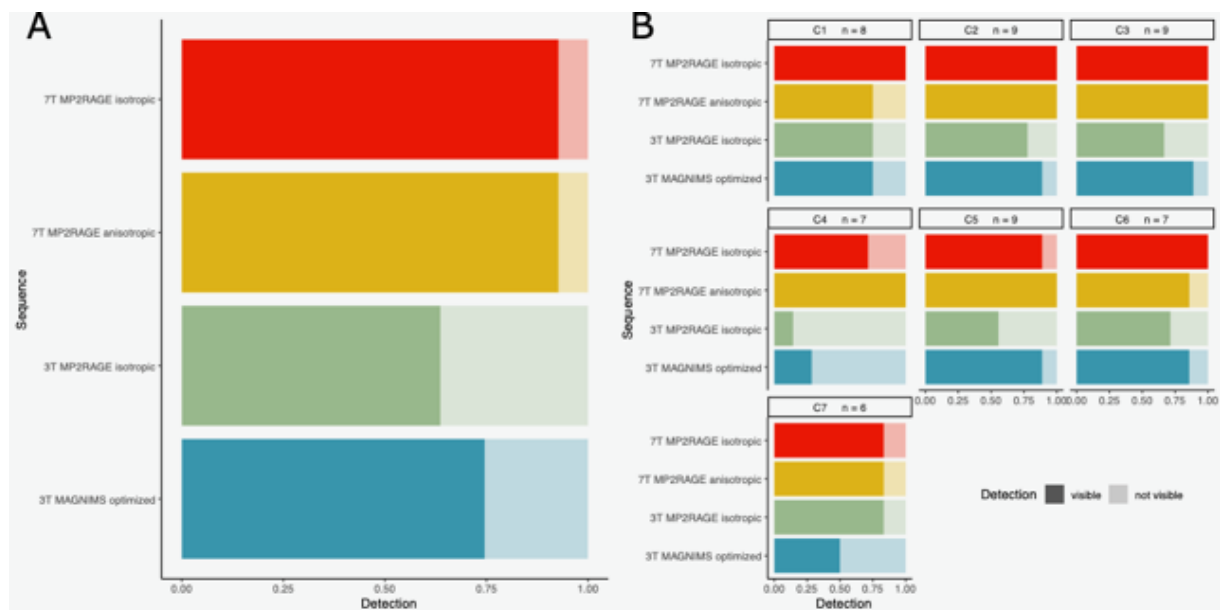


Figure 1: (A) Proportion of lesion detection by sequence and (B) by sequence per vertebral level, for the patients having the 4 imaging sets (14 patients). The number of lesions (n) is detected for each cervical level.

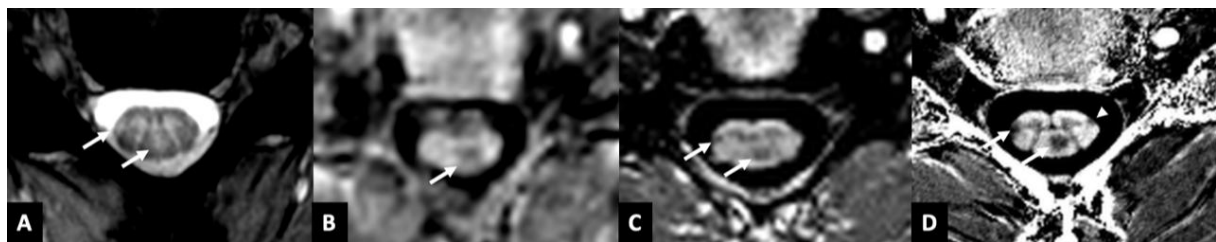


Figure 2: Axial presentation at the C4 level for patient P11. Images were acquired with the T2*GRE-WI (A), 3T UNI-MP2RAGE (B), 7T isotropic UNI-MP2RAGE (C) and 7T anisotropic UNI-MP2RAGE (D) sequences. The posterior lesion was visible on each image, the right lateral lesion was not visible on the 3T UNI-MP2RAGE sequence (B), and the left lateral lesion (white arrowhead) was only detected with the 7T anisotropic UNI-MP2RAGE sequence (D).

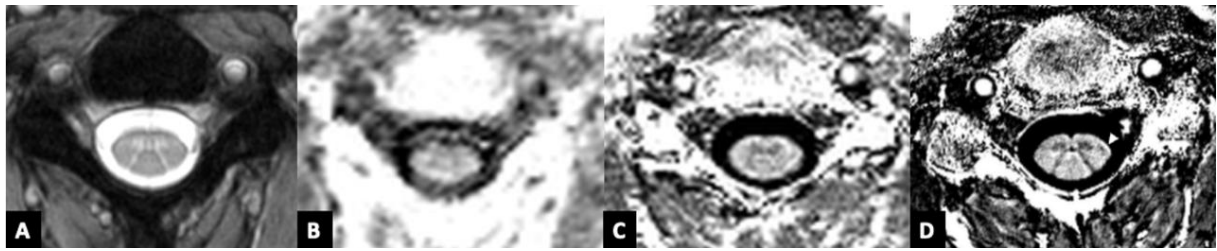


Figure 3: Patient P13 presenting a C4 left lateral lesion (arrowhead). The lesion was not detected on axial T2*GRE-WI image (A), 3T UNI-MP2RAGE (B) nor 7T isotropic UNI-MP2RAGE (C). It was only detected using the 7T anisotropic UNI-MP2RAGE (D).

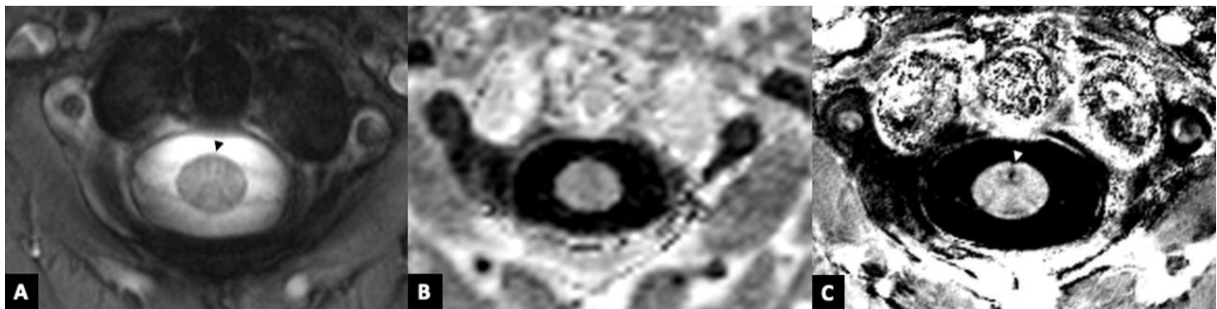


Figure 4: Patient P17 presenting with a small lesion (arrowhead) in contact with the anterior fissure of the spinal cord at C1-C2 level. The lesion was seen on T2*GRE-WI (A) image, not seen on 3T UNI-MP2RAGE (B) and easily seen on 7T UNI-MP2RAGE anisotropic (C) image.

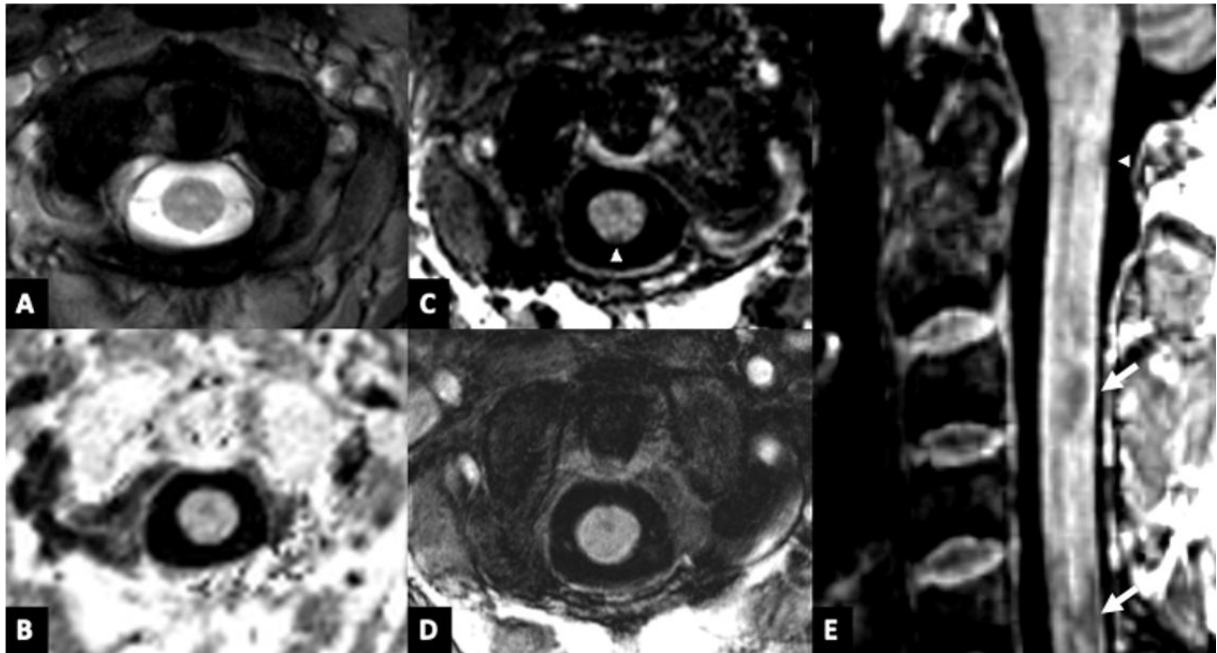


Figure 5: Patient P3 presenting with a small posterior lesion (white arrowhead) at the C1 level, that was not seen on axial T2*GRE-WI (A) image nor with the 3T UNI-MP2RAGE (B). At 7T, the lesion was seen on the axial plane of the isotropic UNI-MP2RAGE sequence (C), but it was not seen on the anisotropic 7T UNI-MP2RAGE image (D). Sagittal plane (E) of the 7T isotropic UNI-MP2RAGE sequence shows that this lesion (white arrowhead) has a very small height. This lesion is not seen on the sagittal 3T UNI-MP2RAGE (F). Additional lesions (white arrows) can be seen at C3 and C5 levels on both sagittal planes (E-F).

Table 1 - Main sequence parameters. * placed perpendicular to the cord, ** depending on cord curvature

Table 2: Demographic and clinical characteristics. M: Male, F: Female, RR: relapsing remitting, EDSS: Expanded Disability Status Scale, * indicates the patients who could not have the examination with the 7T isotropic MP2RAGE sequence.

